Chapter

Indenter Shape Dependent Dislocation Actives and Stress Distributions of Single Crystal Nickel during Nanoindentation: A Molecular Dynamics Simulation

Wen-Ping Wu, Yun-Li Li and Zhennan Zhang

Abstract

The influences of indenter shape on dislocation actives and stress distributions during nanoindentation were studied by using molecular dynamics (MD) simulation. The load-displacement curves, indentation-induced stress fields, and dislocation activities were analyzed by using rectangular, spherical, and Berkovich indenters on single crystal nickel. For the rectangular and spherical indenters, the load-displacement curves have a linear dependence, but the elastic stage produced by the spherical indenter does not last longer than that produced by the rectangular indenter. For a Berkovich indenter, there is almost no linear elastic regime, and an amorphous region appears directly below the indenter tip, which is related to the extremely singular stress field around the indenter tip. In three indenters cases, the prismatic dislocation loops are observed on the {111} planes, and there is a sudden increase in stress near the indenter for the Berkovich indenter. The stress distributions are smooth with no sudden irregularities at low-indentation depths; and the stress increases and a sudden irregularity appears with the increasing indentation depths for the rectangular and spherical indenters. Moreover, the rectangular indenter has the most complex dislocation activities and the spherical indenter is next, while very few dislocations occur in the Berkovich indenter case.

Keywords: molecular dynamics simulation, nanoindentation, indenter shape, dislocation, stress distribution

1. Introduction

Nanoindentation is one of the most popular experiments to investigate the behavior of materials at the nanometer scale [1, 2]. Nanoindentation-probed materials' properties are usually different from their macroscopic counterparts and present different deformation mechanisms [3]. The atomistic models can give important qualitative information for the understanding of experimentally observed complex phenomena; especially, they have the indisputable advantage of analyzing the main physical process and micro-mechanisms (dislocation

nucleation and evolution) [4–9]. Many studies have adopted atomistic simulations to probe and understand detailed deformation process and the possible impact factors involved in nanoindentation. For example, Chan et al. [10] studied the size effects of indenter nanohardness using atomistic simulations, and found that nanohardness was inversely proportional to the indenter radius. Imran et al. [11] studied the influence from the indenter velocity and size of the indenter using molecular dynamics (MD) simulations in Ni single crystals. Noreyan et al. [12] carried out MD simulations of nanoindentation of β-SiC to investigate the dependence of the critical depth and pressure for the elastic-to-plastic transition on indentation velocity, tip size, and workpiece temperature. Yaghoobi et al. [13] and Kim et al. [14] conducted MD simulations of nanoindentation on nickel single crystal and nickel bicrystal and discussed the effects of boundary conditions and grain boundary, respectively. Fu et al. [15] and Yuan et al. [16] investigated the effects of twin boundary on hardness, elastic modulus, and dislocation movements during nanoindentation by MD simulations. Fang et al. [17] carried out MD to find that both Young's modulus and hardness become smaller as temperature increases, and elastic recovery is smaller at higher temperatures during nanoindentation. Wu et al. [18] performed MD simulation to investigate the effects of the temperature, loading and unloading velocities, holding time, and composition of Ni-Al alloys on the nanoimprinting lithography process. Hansson [19], Tsuru et al. [20], and Remington's et al. [21] studies indicated that the crystallographic orientation strongly influenced the hardness, load for pop-in formation, and mechanisms of plastic deformation using nanoindentation simulated by MD. Zhao et al. [22], Chamani et al. [23], and Chocyk et al. [24] also used MD simulation to study nanoindentation behaviors and microstructure features in metallic multilayers, and the effect of layer thickness on nanoindentation hardness was discussed. Furthermore, few studies also found that the geometry shape of indenter have a strong influence on the dislocation nucleation [25, 26], hardness [26, 27], and Young's modulus [27]. Generally, in the MD simulation of nanoindentation, the material properties response is influenced by some factors including specimen thickness, crystal orientation, grain size and boundaries, atomic potentials, boundary conditions, temperature, shape and size of indenter, and loading/unloading rate of indentation, etc.

Although the atomic simulation of nanoindentation process and the influence of different factors have been considered comprehensively, most of them mainly consider the dislocation nucleation and deformation mechanisms of specimen, whereas seldom consider the evolutions of and microstructure and stress field of specimen caused by indenter tip geometry. Especially, the internal relationship between the microstructural evolution and the distribution of stress field during nanoindentation has not been analyzed. Since the microstructure features and its evolutions in a localized region are closely related to the stress field in this region, the mechanical properties are strongly dependent on the microstructural features and their evolutions; and it is important to investigate the microstructure evolution and relation with the local stress field, which can be a great help for further understanding of the physical mechanisms during nanoindentation.

The objective of this contribution is to examine how the development of dislocation microstructures, stress distributions, and load-displacement curves are affected by complex stress sites from different shapes of indenters, to determine the relationships between dislocation microstructures and stress distributions during nanoindentation. Moreover, the effect of shapes of indenters on dislocation nucleation, and dislocation movements, stress distribution characteristics during nanoindentation of single crystal nickel are studied in detail.

2. Simulation procedure and stress calculation

In this work, an open source code LAMMPS [28] is used to carry out MD simulations and investigate the influences of indenter geometry on dislocation movements and stress distributions for a Ni single crystal nanoindentation. Three indenters with different geometries are employed: spherical, rectangular, and Berkovich indenters. The geometries of the models with three different shapes of indenters are shown in **Figure 1**. Both models are in the cubic orientation (i.e., *X*-[100], *Y*-[010], and *Z*-[001]), and the size of box ($X \times Y \times Z$) is 200 Å × 200 Å × 50 Å). A free boundary condition was applied on the top surface of z direction, while the last two layers (7.04 Å) at the bottom of z direction were frozen down, resembling a hard substrate. Periodic boundary conditions (PBC) were applied in the x and y directions, and the sizes of x and y directions, which are perpendicular to the z direction (indentation direction) were chosen to be large enough to avoid spurious effects of the PBC. In the present MD simulations, the embedded-atom-method (EAM) potential provided by Mishin et al. [29] was used, which has previously been successfully applied to simulate FCC single crystal nickel [30, 31]. Atoms in the indenter were kept fixed (indenter was assumed to be an infinitely rigid body), at the start of the simulation, all the models with different indenters are relaxed with the conjugate gradient method to reach a minimum energy state, and then the indenters are inserted into the free top surface of z direction at an average indentation speed of v = 0.25 m/s to a maximum penetration of 15 Å by using a displacement control, and this maximum depth is 30% of the specimen in z direction. When the indenter reaches the maximum depth, the indenter returns to the original position by unloading, hence the indentation process is completed. In addition, to reduce temporal local stress fluctuations, the systems are allowed to relax 4 ps after every increment of the indenters. Meanwhile, considering the time scale limitation of the MD simulation on a nanoindentation procedure, a very low temperature of 1 K is chosen to carry out all nanoindentation simulations, where the indentation rate does not play a significant role as long as it is less than the speed of sound [32]. In the present study, the atomic configurations and their evolutions are analyzed by common neighbor analysis (CNA) proposed by Honeycutt and Andersen [33], because CNA can provide an effective filtering method to classify

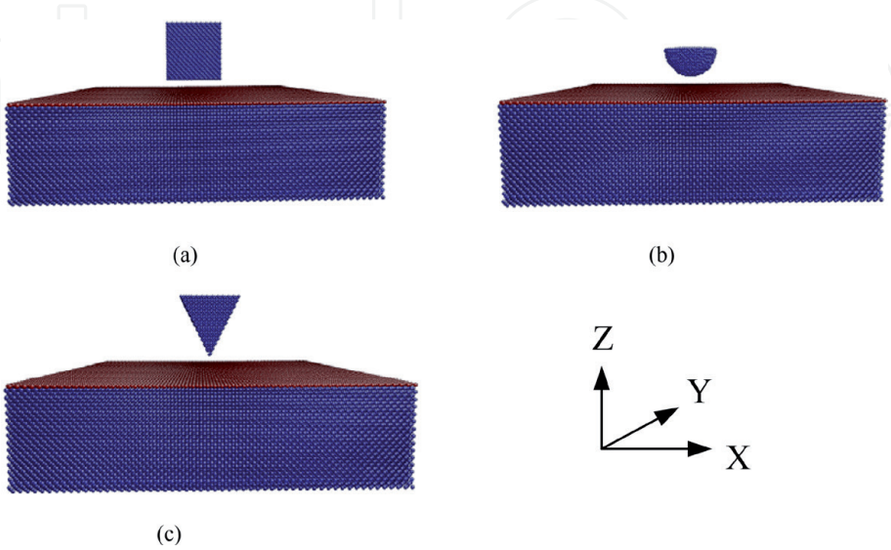

Figure 1.
The geometries of the models with three different shapes of indenters: (a) rectangular indenter, (b) spherical indenter, and (c) Berkovich indenter.

atoms and characterize the local structural environment in crystalline systems. Finally, the atomic configurations and their evolutions are observed by the visualization tools, AtomEye [34], which provides details of the microstructural evolution of nanoindentation.

To investigate the variation and distribution characteristics of atomic stress fields during nanoindentation, the atomistic stress definition is employed in this work. The stress tensor for an atom is calculated as a time averaged value over a number of time steps after relaxation of an indentation step, for atom α of the atomic stress tensor is defined as [35, 36]:

$$\sigma_{ij}^{\alpha} = -\frac{1}{V^{\alpha}}\left(M^{\alpha}v_i^{\alpha}v_j^{\alpha} + \sum_{\beta} F_i^{\alpha\beta} r_j^{\alpha\beta}\right) \quad (1)$$

where V^{α} is the volume of atom α, M^{α} is atomic mass, v_i and v_j are the atom velocity components, and $F_i^{\alpha\beta}$ and $r_j^{\alpha\beta}$ is the force and distance between atoms α and β, respectively.

3. Simulation results and discussion

3.1 Effect of indenter shapes on load: Displacement curves

In order to compare the load-displacement curves of three different indenters, we gave three indenters penetrating into the same maximum indentation depth of 1.5 nm; the load-displacement curves for three different indenters are shown in **Figure 2**. As the indenters are −1 nm away from the contact surface of the specimen surface at the initial stage, the load-displacement is close to a straight line, and the load P is zero for three different shapes of indenter before the separation is approximately −0.5 nm. When the distance between the indenter and the contact surface of the specimen is about −0.5~0 nm, the load values are negative because of the repulsive force of the interaction between atoms, and the repulsive force is larger at the larger contact surface. The rectangular indenter has a larger contact surface than the spherical and Berkovich indenters, the repulsive force is biggest

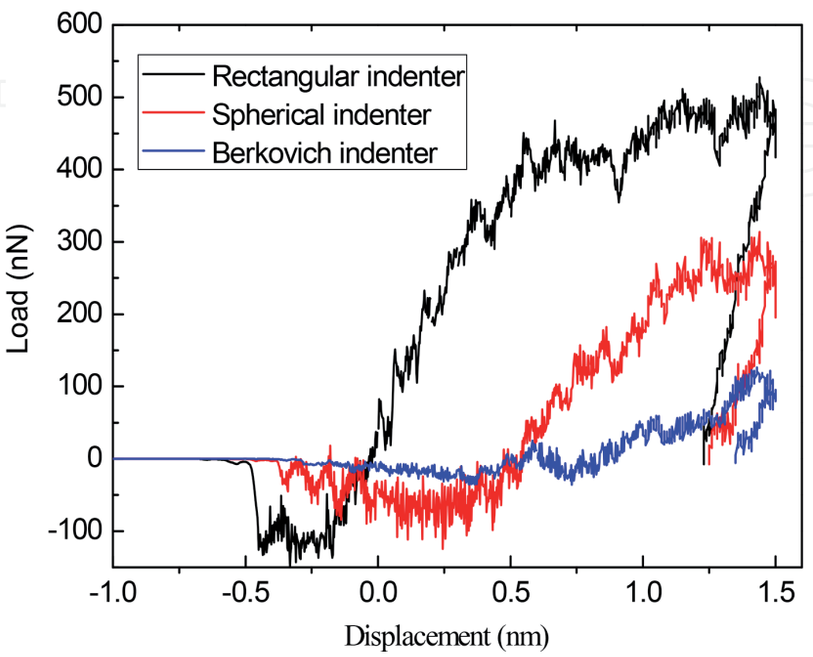

Figure 2.
Load-displacement curves for different shape indenters.

for the rectangular indenter and smallest for the Berkovich indenter (see **Figure 2**). After the indenter contact the surface of the specimen, the load gradually increases with the increase of the penetration depth, the load-displacement curve has a linear dependence, which means that at this stage, the indentation is performed in the linear elastic regime.

For a rectangular indenter, when the load-displacement curve reaches the maximum load, the load keeps fluctuating around a constant value during the further displacement of the indenter, because of the constant cross section of the rectangular indenter; its further penetration into the crystal does not affect significantly the force acting on the indenter. The fluctuations are caused by the relaxation of stresses in the system, such as dislocations migration from the deformed sites. For the spherical indenter, similar to the rectangular indenter case, a quasi-elastic behavior is observed between inflection points; the force acting on the indenter gradually increases with the increase of the penetration depths, but does not last as long in increasing load periods. For a Berkovich indenter, the force acting on the indenter slowly increases with the increase of the penetration depths, the load drop events tend to be small or not noticeable.

Comparison with these three different indenters, the load-displacement curves show different peak loads, elastic-plastic behavior, and load drop events, which are related to a series of transitions of the dislocation structures under the indentation site. To explain this phenomenon, we analyze the local stress distribution and microstructure evolution features of specimen under the indentation site during nanoindentation.

3.2 Effect of indenter shapes on stress distributions

Figure 3 shows atomic stress as a function of atom position along the X direction for different shape indenters during nanoindentation. Here, four different nanoindentation sites are chosen to analyze the atomic stress distributions under the action of different indenters. For rectangular indenter, when indenter does not contact specimen surface [initial site (1) in **Figure 3a**], the atomic stress values are approximately zero along the X direction for three different shape indenters. When the indenter just contacts specimen surface [just contact site (2) in **Figure 3a**], near the contact point, the stress value is positive and relatively high. Whereas the specimen surface at a distance from the contact point, the stress value is negative because the atomic interaction force is repulsive. As the indenter gradually penetrates into the specimen, the stress increases and a sudden irregularity appears. When indenter reaches the maximum indentation depth site (3), the stress value at this site is the highest, and a sudden increase occurs at the indenter site. When the indenter is fully unloaded to the initial site (4) in **Figure 3a**, comparison with the maximum indentation depth, the stress value decreases, but it is still high, which indicates that there are still dislocations in the unloaded specimens and cannot be restored completely. For spherical and Berkovich indenters, a similar trend is found with initially smooth stress distributions, becoming irregular at larger indentation depths. By comparing the stress distributions for three different shape indenters, we found that different indenters have similar stress distribution characteristics at different indentation depth sites, but the stress values are different. The rectangular indenter have the highest stress value (about 6.8 GPa), the spherical indenter is next (about 5.0 GPa), which also has a high stress value (nearly 5.0 GPa) for the Berkovich indenter at the same maximum indentation depth of 1.5 nm. Although the load is the smallest for the Berkovich indenter from the load-displacement curves in **Figure 2**, the contact area of the indenter is also the smallest, resulting in the stress value that is still high near the indenter. It is noteworthy that for the Berkovich indenter, except for the

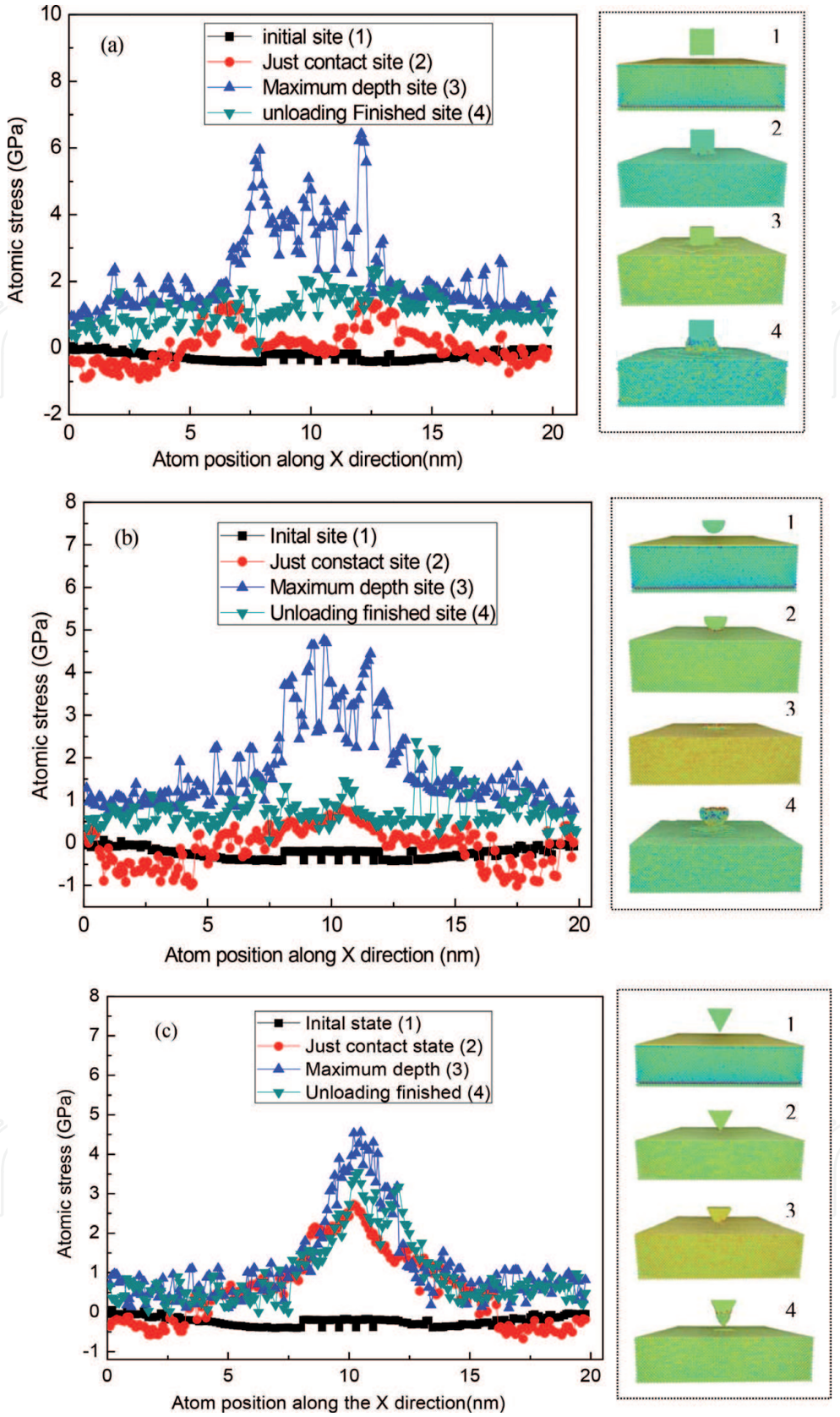

Figure 3.
Atomic stress as function of atom position along the X direction at four different nanoindentation sites for different shape indenters: (a) rectangular indenter, (b) spherical indenter, and (c) Berkovich indenter. The 1, 2, 3, and 4 inserted in figure indicate the indenter at four different nanoindentation sites: (1) initial site (indenter does not contact Ni single crystal specimen), (2) just contact site, (3) maximum depth site, and (4) unloading finished site.

high stress (nearly 5.0 GPa) near the indenter, the other parts of the specimen are very low, which is also the reason for the stress concentration of the sharp indenter. From **Figure 3**, we can see that a sudden increase in stress near the indenter for the

Berkovich indenter, while for the rectangular and spherical indenters, the stress distributions at low indentation depths are smooth with no sudden irregularities, indicating a fully elastic response. At larger indentation depths, the stress distribution gets more and more irregular with locally very high stresses. The stress irregular distribution and the formation of pop-in are closely related to dislocation activities during nanoindentation.

3.3 Effect of indenter shapes on surface and internal microstructures of specimen

To understand the microstructure evolution of the specimen during nanoindentation process, the surface and internal microstructure characteristics of specimen for different shape indenters are presented at the maximum indentation depth site and unloading finished site, as shown in **Figures 4** and **5**, respectively.

Due to the maximum stress and irregular distribution occurring at the maximum indentation depth site, and the dislocation activity is also the most complex at this site, From **Figure 4**, at the same maximum indentation depth of 1.5 nm, we can clearly see that the dislocation structure is the most complex for the rectangular indenter case, and the next for the spherical indenter case, whereas there are only few dislocations for the Berkovich indenter case. Compared to the dislocation activities of rectangular and spherical indenter cases, an amorphous region directly below the indenter tip is observed in the Berkovich indenter case, which we think that the extremely singular stress field around the indenter tip contributes to this uncommon observation.

When the unloading is finished, the indenter returns to its initial site, the stress cannot be completely restored and there are still a lot of dislocations on the surface of the specimen for the rectangular and spherical indenters cases, and these dislocations move slowly toward the surface and boundary of the specimen during unloading, forming the surface microstructure of the specimen as shown in **Figure 5a,b**, while in the Berkovich indenter case, there are almost no dislocations on the surface of specimen at unloading finished site (see **Figure 5c**).

Furthermore, for all three indenters cases at the same maximum indentation depth, the prismatic dislocation loops are mainly observed to nucleate on the {111} planes, as seen the red cycles in **Figures 4** and **5**, this observation in accordance with the predictions of dislocation theory in a face-centered cubic metal. In the rectangular indenter case, dislocation activities are found to be complex; a

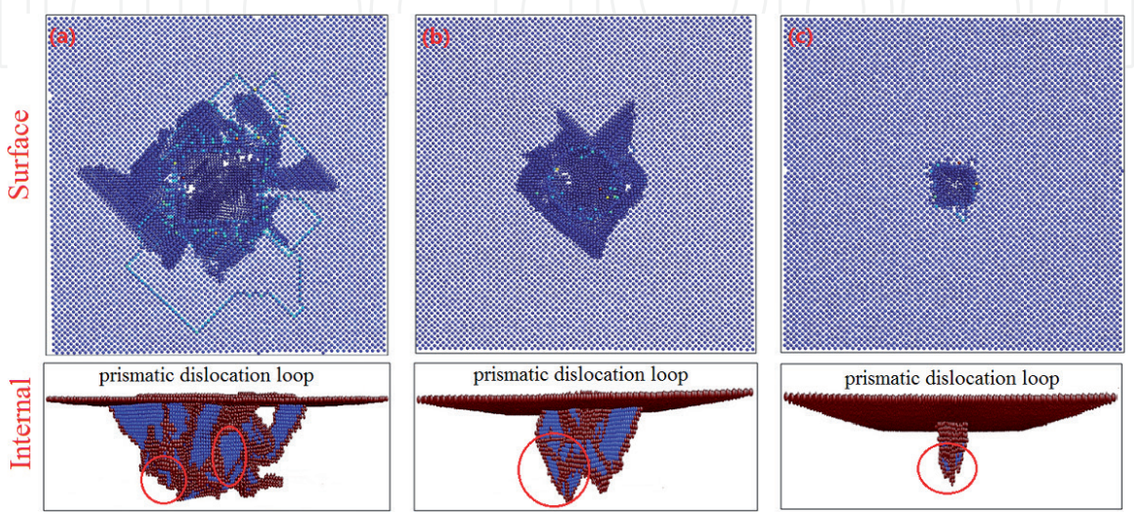

Figure 4.
The surface and internal microstructure features of specimens at maximum depth site for different shape indenters: (a) rectangular indenter, (b) spherical indenter, and (c) Berkovich indenter.

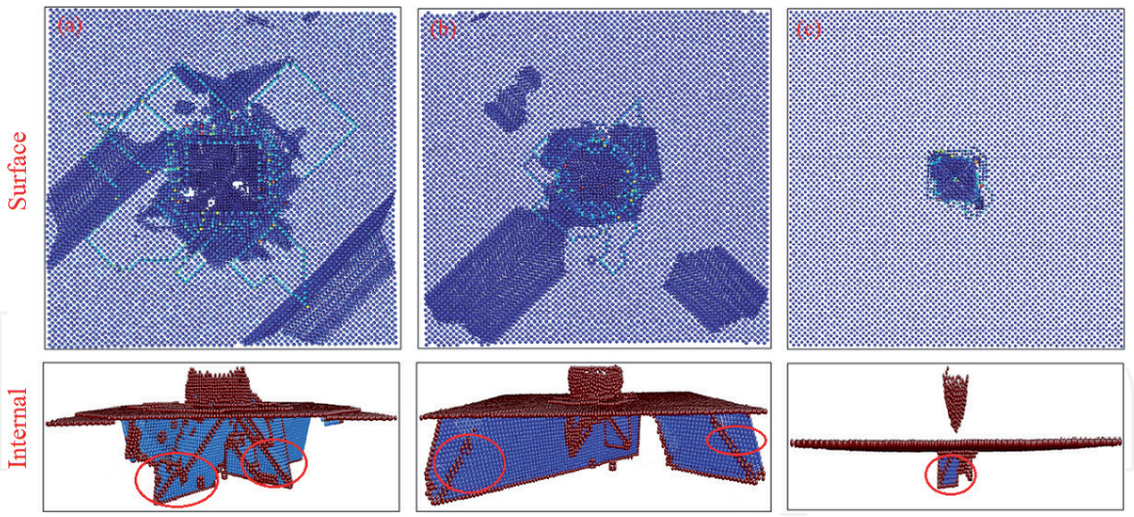

Figure 5.
The surface and internal microstructure features of specimen at unloading finished site for different shape indenters: (a) rectangular indenter, (b) spherical indenter, and (c) Berkovich indenter.

prismatic loop originating inside the specimen is observed and glided upward to the indenting surface. In the spherical indenter case, dislocation activities are still relatively complex, a prismatic dislocation loop originating from the surface of specimen is observed and glided downward to the boundary of specimen. In the Berkovich indenter case, dislocation activities are relatively scarce and the defect structure does not change significantly.

4. Conclusions

MD simulations are performed to investigate the influences of indenter geometry on the dislocation activities and stress distributions during nanoindentation on nickel single crystal. The stress field and dislocation activities induced by the change of indenter shape are analyzed. The major findings are as follows:

1. Load-displacement curves show different peak loads, elastic-plastic behavior, and load drop events in all three cases. For the rectangular and spherical indenters, the load-displacement curves have a linear dependence, which means a linear elastic regime in indentation process, but the elastic stage produced by the spherical indenter does not last long than that produced by the rectangular indenter. For a Berkovich indenter, there is almost no linear elastic regime, the load drop events tend to be small or not noticeable.

2. For the rectangular and spherical indenters, the stress distributions at low indentation depths are smooth with no sudden irregularities, indicating a fully elastic response. At larger indentation depths, the stress distribution becomes more and more irregular with locally very high stresses. For the Berkovich indenter, a sudden increase in stress near the indenter, and the other parts of the specimen is very low, which is the reason for the stress concentration of the sharp indenter. These irregular stress distributions and the formations of pop-in occurred are closely related to dislocation activities during nanoindentation.

3. In all three cases, prismatic dislocation loops are observed to nucleate on the {111} planes, which is in agreement with the predictions of dislocation theory

in a face-centered cubic metal. The dislocation activities are the most complex for the rectangular indenter case, and the next for the spherical indenter case, whereas very few dislocations and an amorphous region directly below the indenter tip are observed in the Berkovich indenter case, which is related to the extremely singular stress field around the indenter tip. According to these results, we can conclude that the shapes of indenters have different and significant influences on dislocation activities and stress distributions during nanoindentation.

Acknowledgements

The work was supported by National Natural Science Foundation of China (Grant Nos. 11772236, 11711530643, and 11472195).

Author details

Wen-Ping Wu[1,2*], Yun-Li Li[1,2] and Zhennan Zhang[1,2]

1 Department of Engineering Mechanics, School of Civil Engineering, Wuhan University, Wuhan, China

2 State Key Laboratory of Water Resources and Hydropower Engineering Science, Wuhan University, Wuhan, China

*Address all correspondence to: wpwu@whu.edu.cn

References

[1] Fischer-Cripps AC. Nanoindentation. 3rd ed. New York, USA: Spring-Verlag; 2011

[2] Schuh CA. Nanoindentation studies of materials. Materials Today. 2006;**9**(5):32-40

[3] Kiely JD, Houston JE. Nanomechanical properties of Au (111), (001), (110) surface. Physical Review B. 1998;**57**:12588

[4] Li J, Vliet KJV, Zhu T, Yip S, Suresh S. Atomistic mechanism governing elastic limit and incipient plasticity in crystals. Nature. 2002;**418**:307-310

[5] Lee Y, Park JY, Kim SY, Jun S, Im S. Atomistic simulations of incipient plasticity under Al (111) nanoindentation. Mechanics of Materials. 2005;**37**:1035-1048

[6] Liang HY, Woo CH, Huang H, Ngan AHW, Yu TX. Dislocation nucleation in the initial stage during nanoindentation. Philosophical Magazine. 2003;**83**:3609-3622

[7] Lilleodden ET, Zimmerman JA, Foiles SM, Nix WD. Atomistic simulations of elastic deformation and dislocation nucleation during nanoindentation. Journal of the Mechanics and Physics of Solids. 2003;**51**(5):901-920

[8] LuZ, Chernatynskiy A, Noordhoek MJ, Sinnott SB, Phillpot SR. Nanoindentation of Zr by molecular dynamics simulation. Journal of Nuclear Materials. 2015;**467**:742-757

[9] DaSilva CJ, Rino JP. Atomistic simulation of the deformation mechanism during nanoindentation of gamma titanium aluminide. Computational Materials Science. 2012;**62**:1-5

[10] Chan CY, Chen YY, Chang SW, Chen CS. Atomistic studies of nanohardness size effects. International Journal of Theoretical and Applied Multiscale Mechanics. 2011;**2**(1):62-71

[11] Imran M, Hussain F, Rashid M, Ahmad SA. Dynamic characteristics of nanoindentation in Ni: A molecular dynamics simulation study. Chinese Physics B. 2012;**21**(11):116201

[12] Noreyan A, Amar JG, Marinescu I. Molecular dynamics simulations of nanoindentation of β-SiC with diamond indenter. Materials Science and Engineering B. 2005;**117**:235-240

[13] Yaghoobi M, Voyiadjis GZ. Effect of boundary conditions on the MD simulation of nanoindentation. Computational Materials Science. 2014;**95**:626-636

[14] Kim KJ, Yoon JH, Cho MH, Jang H. Molecular dynamics simulation of dislocation behavior during nanoindentation on a bicrystal with a Σ=5 (210) grain boundary. Materials Letters. 2006;**60**:3367-3372

[15] Fu T, Peng X, Chen X, Wen S, Hu N, Li Q, et al. Molecular dynamics simulation of nanoindentation on Cu/Ni nanotwinned multilayer films using a spherical indenter. Scientific Reports. 2016;**6**:35665

[16] Yuan L, Xu Z, Shan D, Guo B. Atomistic simulation of twin boundaries effect on nanoindentation of Ag (111) films. Applied Surface Science. 2012;**258**:6111-6115

[17] Fang TH, Weng CI, Chang JG. Molecular dynamics analysis of temperature effects on nanoindentation measurement. Materials Science and Engineering A. 2003;**357**:7-12

[18] Wu CD, Fang TH, Sung PH, Hsu QC. Critical size, recovery, and

mechanical property of nanoimprinted Ni-Al alloys investigation using molecular dynamics simulation. Computational Materials Science. 2012;**53**:321-328

[19] Hansson P. Influence of the crystallographic orientation and thickness of thin copper coatings during nanoindentation. Engineering Fracture Mechanics. 2015;**150**:143-152

[20] Tsuru T, Shibutani Y. Anisotropic effects in elastic and incipient plastic deformation under (001), (110) and (111) nanoindentation of Al and Cu. Physical Review B. 2007;**75**:035415

[21] Remington TP, Ruestes CJ, Bring EM, Remington BA, Lu CH, Kad B, et al. Plastic deformation in nanoindentation of tantalum: A new mechanism for prismatic loop formation. Acta Materialia. 2014;**78**:378-393

[22] Zhao Y, Peng X, Fu T, Sun R, Feng C, Wang Z. MD simulation of nanoindentation on (001) and (111) surfaces of Ag–Ni multilayers. Physica E. 2015;**74**:481-488

[23] Chamani M, Farrahi GH, Movahhedy MR. Molecular dynamics simulation of nanoindentation of nanocrystalline Al/Ni multilayers. Computational Materials Science. 2016;**112**:175-184

[24] Chocyk D, Zientarski T. Molecular dynamics simulation of Ni thin films on Cu and Au under nanoindentation. Vacuum. 2018;**147**:24-30

[25] Lai CW, Chen CS. Influence of indenter shape on nanoindentation: An atomistic study. Interaction and Multiscale Mechanics. 2013;**6**(3):301-306

[26] Voyiadjis GZ, Yaghoobi M. Large scale atomistic simulation of size effects during nanoindentation: Dislocation length and hardness. Materials Science and Engineering A. 2015;**634**:20-31

[27] Verkhovtsev AV, Yakubovich AV, Sushko GB, Hanauske M, Solov'yov AV. Molecular dynamics simulations of the nanoindentation process of titanium crystal. Computational Materials Science. 2013;**76**:20-26

[28] Plimpton SJ. Fast parallel algorithms for short-range molecular dynamics. Journal of Computational Physics. 1995;**117**:1-19. Available at: http://lammps.sandia.gov/

[29] Mishin Y, Farkas D, Mehl MJ, Papaconstantopoulos DA. Interatomic potentials for monatomic metals from experimental data and ab initio calculations. Physical Review B. 1999;**59**:3393-3407

[30] Nair AK, Parker E, Gaudreau P, Farkas D, Kriz RD. Size effects in indentation response of thin films at the nanoscale: A molecular dynamics study. International Journal of Plasticity. 2008;**24**:2016-2031

[31] Karimi M, Roarty T, Kaplan T. Molecular dynamics simulations of crack propagation in Ni with defects. Modelling and Simulation in Materials Science and Engineering. 2006;**14**:1409-1420

[32] Shi Y, Falk ML. Stress-induced structural transformation and shear banding during simulated nanoindentation of a metallic glass. Acta Materialia. 2007;**55**:4317-4324

[33] Honeycutt JD, Andersen HC. Molecular dynamics study of melting and freezing of small Lennard-Jones clusters. The Journal of Physical Chemistry. 1987;**91**:4950-4963

[34] Li J. Atomeye: An efficient atomistic configuration viewer. Modelling and Simulation in Materials Science and Engineering. 2003;**11**:173-177

[35] Born M, Huang K. Dynamical Theory of Crystal Lattices. Clarendon Press, Oxford; 1954

[36] Horstemeyer MF, Baskes MI. Atomistic finite deformation simulations: A discussion on length scale effects in relation to mechanical stresses. Journal of Engineering Materials and Technology. 1999;**121**:114-119